Networking Working Group
Internet-Draft
Intended status: Informational
Expires: July 12, 2011

J. Tripathi, Ed.
J. de Oliveira, Ed.
Drexel University
JP. Vasseur, Ed.
Cisco Systems, Inc.
January 11, 2011

Performance Evaluation of Routing Protocol for Low Power and Lossy Networks (RPL)

draft-tripathi-roll-rpl-simulation-06

Abstract

This document presents a performance evaluation of the Routing Protocol for Low power and Lossy Networks (RPL) for a small outdoor and for a large scale smart meter network. Detailed simulations are carried out to produce several routing performance metrics using a set of real-life scenarios.

Status of this Memo

Copyright Notice

Contents

1 Terminology

Please refer to the following document for terminology in [I-D.ietf-roll-terminology]. In addition, the following terms are specified:

- PDR : Packet Delivery Ratio.
- CDF : Cumulative Distribution Function describes the probability that a real-valued random variable X with a given probability distribution will be found at a value less than or equal to x. Mathematically, CDF of X is $F(X) = P(X \leq x)$.
- Fractional Stretch Factor of link ETX Metric against ideal shortest path: The ETX path stretch is defined as the difference between the number of expected transmissions (ETX Metric) taken by a packet traveling from source to destination, following a route determined by RPL and a route determined by a hypothetical ideal shortest path routing protocol (using link ETX as the metric). The fractional path stretch is the ratio of ETX path stretch to ETX path cost for the shortest path route for that source-destination pair.
- Stretch factor for node hop distance against ideal shortest path: The hop stretch is defined as the difference between the number of hop counts taken by a packet traveling from source to destination, following a route determined by RPL and by a hypothetical ideal shortest path algorithm, both using ETX as the link cost. The fractional stretch factor is computed as the ratio of path stretch to count value between a source-destination pair for the hypothetical shortest path route optimizing ETX path cost.

2 Introduction

Designing a routing protocol for Low power and Lossy link Networks (LLNs) imposes great challenges, mainly due to low data rates, high probability of packet delivery failure, and strict energy constraint in nodes. The IETF ROLL Working Group took on this task and specified the Routing Protocol for Low power and Lossy Networks (RPL) in [I-D.ietf-roll-rpl].

RPL is designed to meet the core requirements specified in [RFC5826],[RFC5867],[RFC5873] and [RFC5548].

This document's contribution is to provide a performance evaluation of RPL with respect to several metrics of interest. This is acomplished using real data and topologies in a discrete event simulator developed to reproduce the protocol behavior.

The following metrics are evaluated in this document:

- Path quality metrics;
- Control plane overhead;
- End to End delay between nodes.
- Ability to cope with unstable situations (link churns, node dying);
- Required resource constraints on nodes (routing table size, etc.).

Feedback from the ROLL Working Group are welcome to add new evaluation metrics of potential interest in further revisions of this document.

Although simulation cannot formally prove that a protocol operates properly in all situations, it can give a good level of confidence in protocol behavior in highly stressful conditions, if and only if real life data are used. Simulation is particularly useful when theoretical model assumptions may not be applicable to such networks and scenarios. In this document, real deployed network data traces have been used to model link behaviors and network topologies.

3 Methodology and Simulation Setup

In the context of this document, RPL has been simulated using OMNET++ [OMNETpp], a well-known discrete event based simulator written in C++ and NED. Castalia-2.2 [Castalia-2.2] has been used as Wireless Sensor Network Simulator framework within OMNET++. The output and events in the simulating are visualized with the help of the Network AniMator or NAM, which is distributed with NS (Network Simulator) [NS-2].

Note that NS or any of its versions are not used in this simulation study. Only the visualization tool was borrowed for verification purposes.

In contrast with theoretical models, which as stated before may have assumptions not applicable to lossy links, real-life data has been used for two aspects of the simulations:
* Link failure model: Time varying real network traces containing packet delivery probability for each link over all channels for both indoor network deployment.
* Topology: Gathered from real-life deployment (traces mentioned above) as opposed to random topology simulations.
A 45 node topology, deployed as an outdoor network, shown in Figure 1 and a 2442 node topology, gathered from a smart meter network deployment, were used in the simulations.

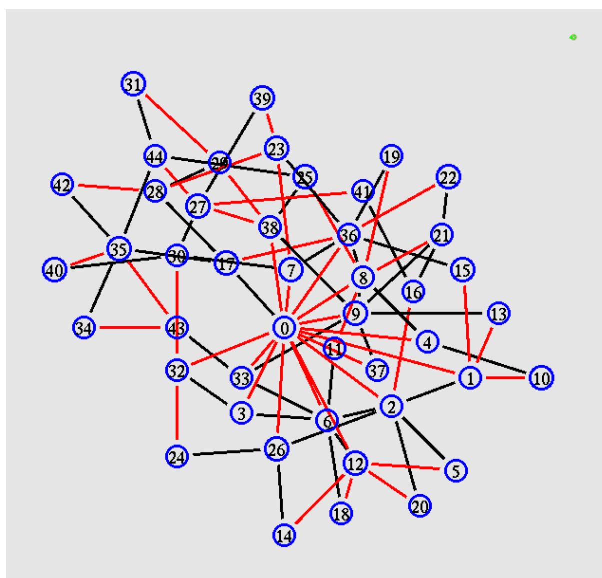

Figure 1: 45 nodes outdoor network topology.

Note that this is just a start to validate the simulation before using large scale networks.

A set of time varying link quality data was gathered from real network deployment to form a database used for the simulations. Each link in the topology 'picks up' the same link model (trace) from the database corresponding to real model in deployment. Each link has a Packet Delivery Ratio (PDR) that varies with time (in the simulation, a new PDR is read from the database every 10 minutes) according to the gathered data. Packets are dropped randomly from that link with probability (1 - PDR). Each time a packet arrives at the Radio of a node, the module generates a random number by the Mersenne Twister Random number generation method. The random number is compared to the PDR to determine whether the packet should be dropped. Note that each link uses a different random number generator to maintain true randomness in the simulator, and to avoid correlation between links. Also, the packet drop applies to all kinds of data and control packets (RPL) such as the DIO, DAO, DIS packets defined in [I-D.ietf-roll-rpl]. Figure 2 shows some typical temporal characteristics of some links in the network for the indoor network traces used in the simulations.

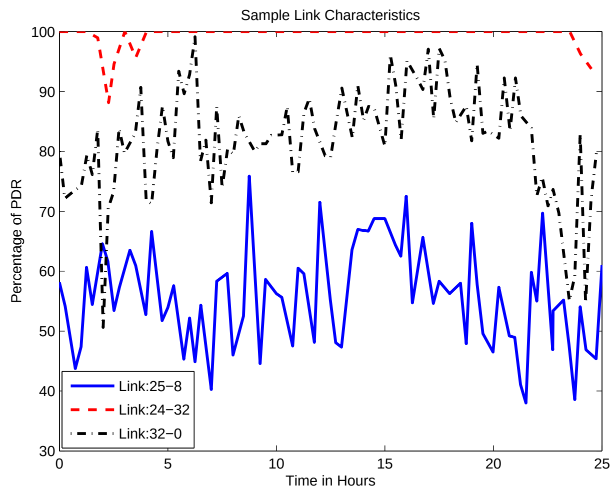

Figure 2: Example of link characteristics.

In the RPL simulator, the LBR first initiates sending out DIO messages, and the DAG is gradually constructed. RPL makes use of trickle tim ers: I_min is initially set to 1 second and I_doubling is equal to 16, so that maximum time between two consecutive DIO emissions by a node (under a steady network condition) is 18.2 hours. The trickle time interval for emitting DIO message assumes the initial value of 1 second, and then changes over simulation time as mentioned in [I-D.ietf-roll-trickle].

Another objective of this study is to give insight to the network administrator on how to tweak the trickle values. These recommendations could then be used in applicability statement documents.

Each node in the network, other than the LBR (Low power and lossy Border Router), also emits DAO messages as specified in [I-D.ietf-roll-rpl], to initially populate the routing tables with the prefixes received from children via the DAO messages to support Point to Point (P2P) and Point to Multipoint traffic (P2MP) in the "down" direction. During these simulations, it is assumed that each node is capable of storing route information for other nodes in the network (storing mode of RPL).

For nodes implementing RPL, as expected, the routing table memory requirement varies according to the position in the DODAG (Destination Oriented Directed Acyclic Graph). The (worst-case) assumption is made that there is no route summarization (aggregation) in the network. Thus a node closer to the DAG will have to store more entries in its routing table. It is also assumed that all nodes have equal memory capacity to store the routing states.

For simulations of the indoor network, each node sends traffic according to a Constant Bit Rate (CBR) to all other nodes in the network, over the simulation period. Each node generates a new data packet every 10 seconds. Each data packet has a size of 127 bytes including 802.15.4 PHY/MAC headers and RPL packet headers. All control packets are also encapsulated with 802.15.4 PHY/MAC headers. To simulate a more realistic scenario, 20% of the generated packets by each node are destined to the root, and the remaining 80% of the packets are uniformly assigned as destined to nodes other than the root.

Therefore the root receives a considerably larger amount of data than other nodes. These values may be revised when studying P2P traffic so as to have a majority of traffic going to all nodes as opposed to the root. In the later part of the simulation, a typical home/ building routing scenario is also simulated, and different path quality metrics are computed for that traffic pattern.

The packets are routed through the DODAG built by RPL according to the mechanisms specified in [I-D.ietf-roll-rpl].

A number of RPL parameters are studied (such as Packet Rate from each source, Time Period of the LBR emitting new DAG Sequence Number) to observe their effect on the performance metric of interest.

4 Performance Metrics

4.1 Common Assumptions

As the DAO messages help to feed the routing tables in the network, they grow with time and size of the network. Nevertheless, no constraint was imposed on the size of the table nor on how much information the node can store. The routing table size is not expressed in terms of Kbyte of memory usage but measured in terms of number of entries for each node. Each entry has the next hop node and path cost associated with the destination node.

The link ETX (Expected Transmission Count) metric is used to build the DODAG. The link ETX routing metric is specified in [I-D.ietf-roll-routing-metrics].

4.2 Path Quality

Number of Hops: For each source-destination pair, the average number of hops for both RPL and shortest path routing is computed. Shortest path routing refers to a hypothetical ideal routing protocol that would always provide the shortest path in term of Total path cost ETX (or whichever metric is used) in the network. The Cumulative Distribution Function (CDF) of hop distance for all paths (n*(n-1) in an n-node network) in the network with respect to the number of hops is plotted in Figure 3 for both RPL and shortest path routing. One can observe that the CDF corresponding to 4 hops is around 55% for RPL and 90% for shortest path routing. In other words, for the given topology, 90% of paths have a path length of 4 hops or less with an ideal shortest path routing methodology, whereas in RPL Point-to-Point (P2P) routing, 90% of the paths will have a length of no more than 5 hops. This result indicates that despite having a non-optimized P2P routing scheme, the path quality of RPL is close to an optimized P2P routing mechanism. Another reason for this may relate to the fact that, the sink is at the center of the network, thus routing through the sink is often close to an optimal (shortest path) routing. This result may be different in a topology where the sink is located at one end of the network.

Path Cost ETX: The path cost ETX of the path is computed for each source-destination pair. In the simulation, the path ETX from source to destination for each packet is computed. Figure 4 shows the CDF of the total path cost ETX, for both RPL and shortest path routing. Here also one can observes that the total path cost ETX from all source to all destinations is close to that of a shortest path routing for the network.

Path Stretch: In this simulation, the path stretch is also calculated for each packet that traversed the network. The path stretch is determined as the difference between the number of hops taken by a packet while following a route built via RPL and the number of hops taken by shortest path routing (using link ETX as the metric).

Once again, the CDF of the path stretch is plotted against the value of path stretch over all packets in Figures 5 and 6, for hop count stretch and ETX metric stretch respectively. It can be observed that for a

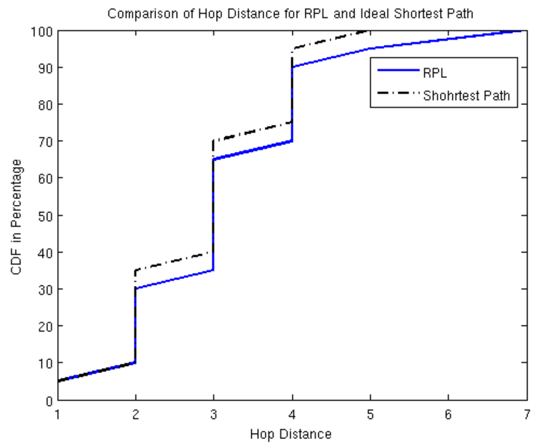

Figure 3: CDF: hop distance versus number of hops.

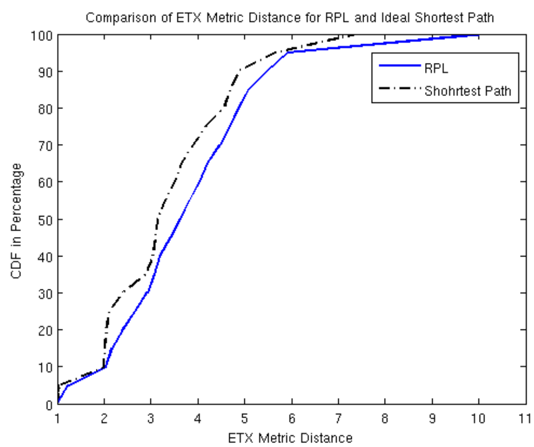

Figure 4: CDF: Total ETX along path versus ETX value.

few packets, path built via RPL has fewer hops than the ideal shortest path where path ETX is minimized along the DAG. This is because there are a few source - destination pairs, where the total path ETX is equal to or less than that of the ideal shortest path when the packet takes a longer hop count. As the RPL implementation ignores 20% change in total path cost before switching to a new parent or emitting new DIO, RPL not necessarily provides the shortest path in terms of total ETX path cost. Thus, this implementation yields a few paths with smaller hop count but larger (or equal) total ETX path cost.

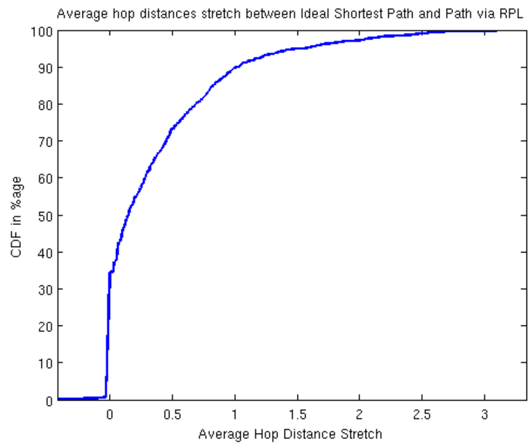

Figure 5: CDF: Hop count stretch versus hop count of a packet.

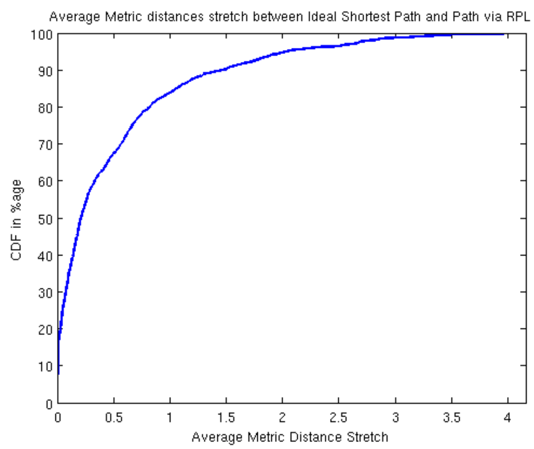

Figure 6: CDF: ETX metric stretch versus ETX value.

4.3 Routing Table Size

The objective of this metric is to observe the distribution of the number of entries per node. Figure 7 shows the CDF of the number of routing table entries for all nodes. Note that 90% of the nodes need to store less than 10 entries in their routing cache.

4.4 Delay bound for P2P Routing

For delay sensitive applications, such as home and building automation, it is also critical to optimize the end-to-end delay. Figure 8 shows the upper bound and distributions of delay for paths between any two given nodes for different hop counts between source and destination. Here, the hop count refers to the the number of hops a packet travels to reach the destination when using RPL paths. This hop distance does not correspond to shortest path distance between two nodes. Note that, each packet has a length of 127 bytes, with a 240 kbps radio, which makes the transmission time approximately 4 ms.

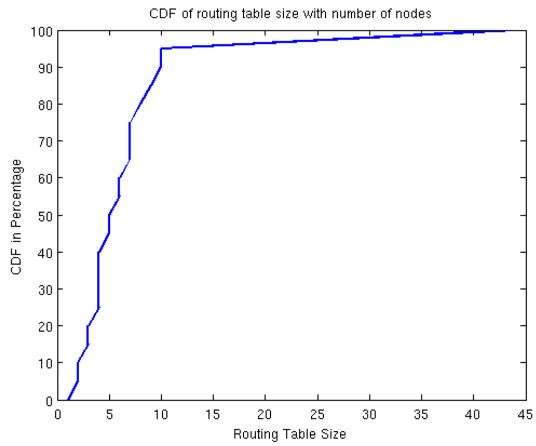

Figure 7: CDF of routing table size with respect to number of nodes.

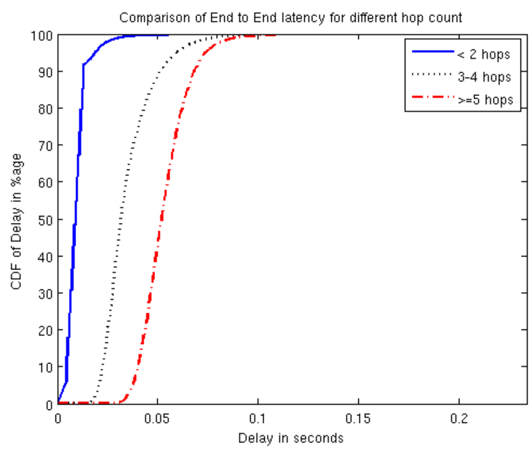

Figure 8: Comparison of packet latency for different path length expressed in hop count.

4.5 Control Packet Overhead

The control plane overhead is an important routing characteristic in LLNs. It is imperative to bound the control plane overhead. One of the distinctive characteristics of RPL is that it makes use of trickle timers so as to reduce the number of control plane packets by eliminating redundant messages. The aim of this performance metric is thus to analyse the control plane overhead both in stable conditions (no network element failure overhead) and in the presence of failures.

Data and control plane traffic comparison for each node: Figure 9 shows the comparison between the amount of data packets transmitted (including forwarded) and control packets (DIO and DAO messages) transmitted for all individual nodes when link ETX is used to optimize the DAG. As mentioned earlier, each node generates a new data packet every 10 seconds. Here one can observe that a considerable amount of traffic is routed through the sink itself. The x axis indicates the node ID in the network. Also, as expected, the nodes closer to sink and that act as routers (as opposed to leaves) handle much more data traffic than other nodes. Looking at a link close to the root, we can observe that the proportion of control traffic is negligible. This result also reinforces the fact that the amount of control plane traffic generated by RPL is negligible. Leaf nodes have comparable amount of data and control packet transmission (they do not take part in routing the data).

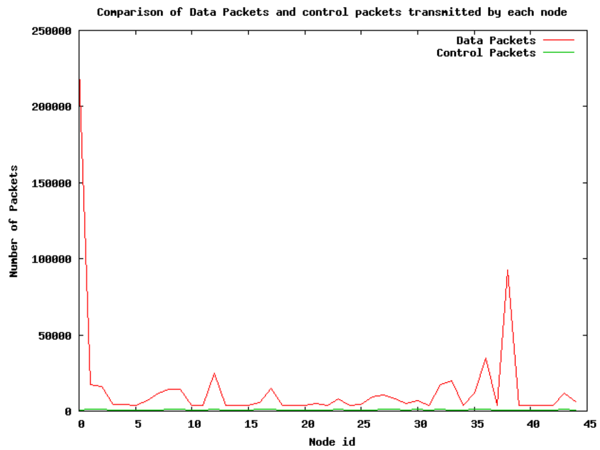

Figure 9: Amount of data and control packets transmitted against node ID using ETX as routing metric.

Data and Control Packet Transmission with Respect to Time: In Figures 10, 11 and 12, the amount of data and control packets transmitted for node 12 (low rank in DAG, closer to the root), node 43 (in the middle) and node 31 (leaf node)are shown, respectively. These values stand for number of data and control packets transmitted for each 10 minute intervals for the particular node, to help understand what is the ratio between data and control packets exchanged in the network. One can observe that nodes closer to the sink have ink, because in each interval the destinations of the packets from same source changes, while 20% of the packets are destined to the sink. As a result, pattern of the traffic handled changes widely in each interval for the nodes closer to the sink. For the nodes that are farther away from sink, the ratio of data and control traffic is smaller since the amount of data traffic is greatly reduced.

The control traffic load exhibits a wave-like pattern. The amount of control packets for each node drops quickly as the DODAG stabilizes due to the effect of trickle timers. However, when a new DODAG sequence is advertised (global repair of the DODAG), the trickle timers are reset and the nodes start emitting DIOs frequently again to rebuild the DODAG. For a node closer to the sink, the amount of data packets is much larger than that of control packets, and somewhat oscillatory around a mean value. The amount of control packets exhibits a 'saw-tooth' behavior. As the ETX link metric was used, when the PDR changes, the ETX link metric for a node to its child changes, which may lead to choosing a new parent, and changing the DAG rank of the child. This event resets the trickle timer and triggers the emission of a new DIO. Also, issue of a new DODAG sequence number triggers DODAG re-computation and resets the trickle timers. Therefore, one can observe that the number of control packets attains a high value for one interval, and comes down to lower values for subsequent intervals. The interval with high value of control packets denote the interval where the timers to emit new DIO are reset more frequently. As the network stabilizes, the control packets are less dense in volume. For leaf nodes, the amount of control packets is comparable to that of data packets, as leaf nodes are more prone to face changes in their DODAG rank as opposed to nodes closer to sink when the link ETX value in the topology changes dynamically.

4.6 Loss of connectivity

Upon link failures, a node may lose his parents: preferred and backup (if any) and its sibling (if any) thus to leading to a loss of connectivity (no path to the DODAG root). In this case, if a packet has to be sent and the routing table does not contain an entry for the corresponding destination the packet is

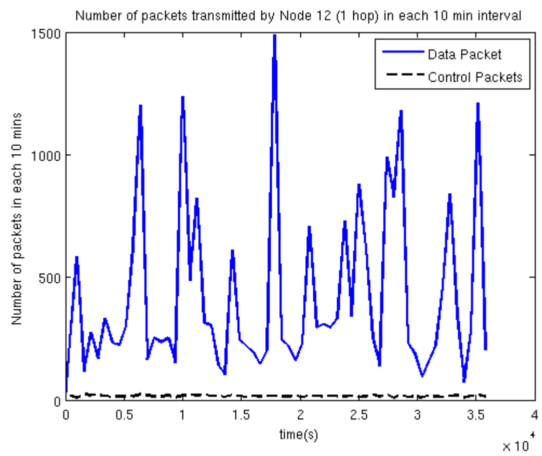

Figure 10: Amount of data and control packets transmitted for node 12.

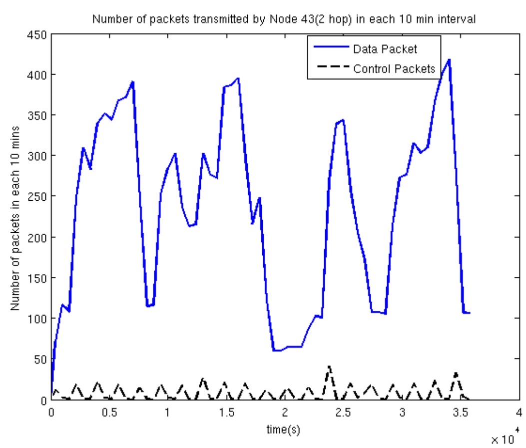

Figure 11: Amount of data and control packets transmitted for node 43.

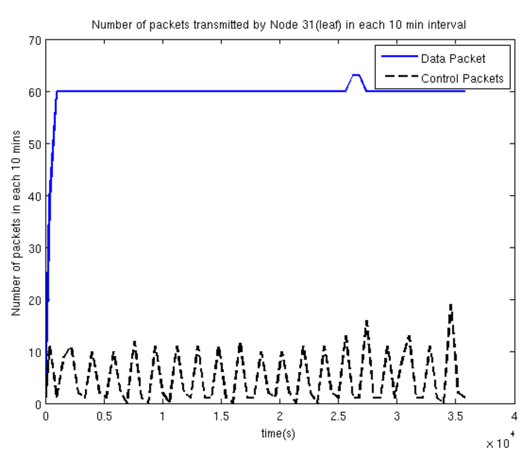

Figure 12: Amount of data and control packets transmitted for node 31.

dropped. RPL specifies two mechanisms for DODAG repairs, referred to as the Global Repair and Local

Repair. In this version of the document, simulation results are presented to evaluate the amount of time data packets are dropped due to a loss of connectivity for the following two cases: *a*) when only using global repair (i.e., the DODAG is rebuilt thanks to the emission of new DODAG sequence numbers by the DODAG root), and *b*) when using local repair (poisoning the sub-DAG in case of loss of connectivity) in addition to global repair. The idea is to tune the frequency at which new DODAG sequence numbers are generated by the DODAG root that are used for global repair, and also to observe the effect of varying the frequency for global repair and the concurrent use of global and local repair. It is expected that more frequent increments of DODAG sequence number will lead to shorter duration of connectivity loss at a price of a higher rate of control packet in the network. For the use of both global and local repair, the simulation results show the trade-off in amount of time that a node may remain without service and total number of control packets for extra bit of signalling.

Figure 13 shows the CDF of time spent by any node without service, when the rate of data packet is one packet every 10 seconds, and new DODAG sequence number is generated every 10 minutes. This plot reflects the property of global repair without any local repair scheme. When all the parents (and siblings) are temporarily unreachable from a node, the time before it hears a DIO from another node is recorded, which gives the time without service. We define DAG repair timer to be the interval at which the LBR increments the DAG sequence number, thus trigerring a global reoptimization. In some cases, this value might go up to the DAG repair timer value, because until a DIO is heard,the node does not have a parent, and hence no route to the LBR or other nodes not in its own sub-DAG. Clearly, this situation indicates a lack of connectivity and loss of service for the node.

The effect of the DAG repair timer on time without any service is plotted in Figure 14, where the source rate is 20 seconds/packet and in Figure 15, where the source sends a packet every 10 seconds.

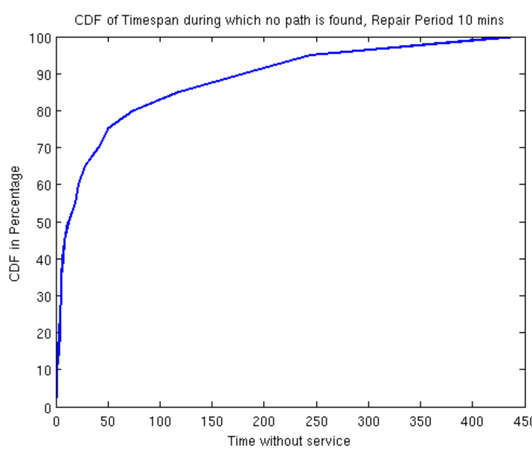

Figure 13: CDF: Loss of connectivity with global repair.

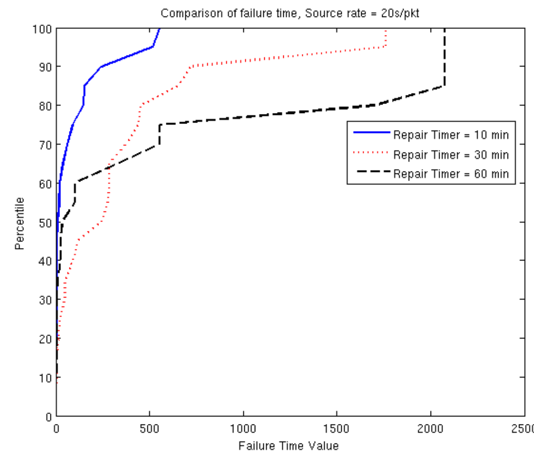

Figure 14: CDF: Loss of connectivity for different global repair period, packet rate 20/s.

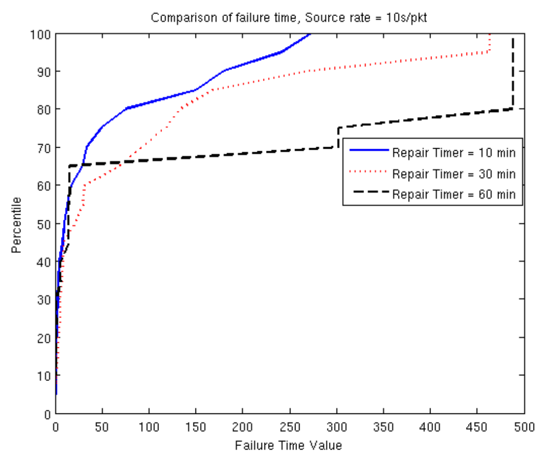

Figure 15: CDF: Loss of connectivity for different global repair period, packet rate 10/s.

Figure 16 shows the effect of DAG global repair timer period on control traffic. As expected, as the frequency at which new DAG sequence number are generated increases, the amount of control traffic decreases because DIO messages are sent less frequently to rebuild the DODAG. However reducing the control traffic comes at a price of increased loss of connectivity when only global repair is used.

The effect of the DAG repair timer on time without service, when local repair is activated, is now observed and is plotted in 17, where the source rate is 20 seconds/packet. A comparison of the CDF of loss of connectivity for global repair mechanism and global + local repair mechanism is shown in Figures 18 and 19 (semilog plots, x axis in logarithmic and y axis in linear scale), where the source generates a packet every 10 seconds and 20 seconds, respectively. For these plots, the x axis shows time in log scale, and y axis denotes the corrsesponding CDF in linear scale. One can observe that using local repair (using poisoning of the sub-DAG) greatly reduces loss of connectivity.

A comparison between the amount of control overhead used for global repair only and global plus local Repair mechanism is shown in Figure 20, which highlights the improved performance of RPL in terms of convergence time at very little extra overhead.

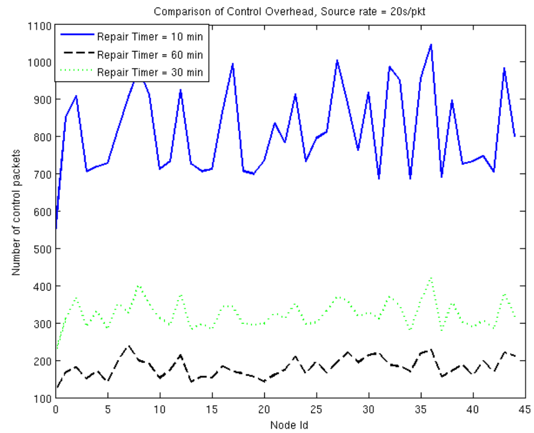

Figure 16: Amount of control traffic for different global repair periods.

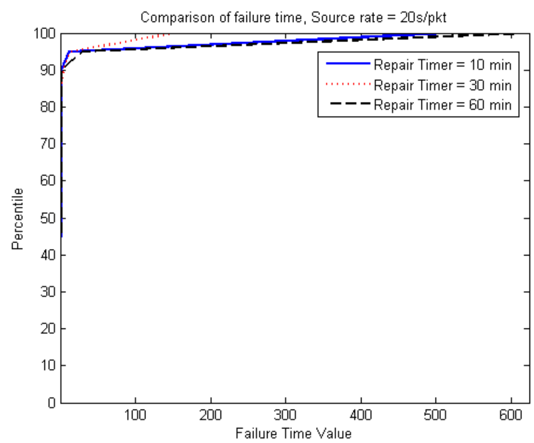

Figure 17: CDF: Loss of connectivity for different DAG repair timer values for gloabal+local repair, packet rate 20/s.

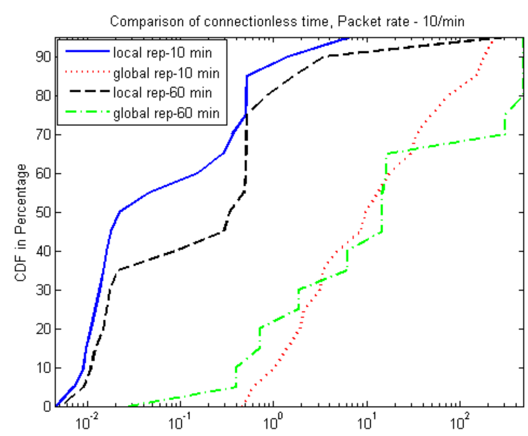

Figure 18: CDF: Comparing loss of connectivity for global repair and global+local repair, packet rate 10/s.

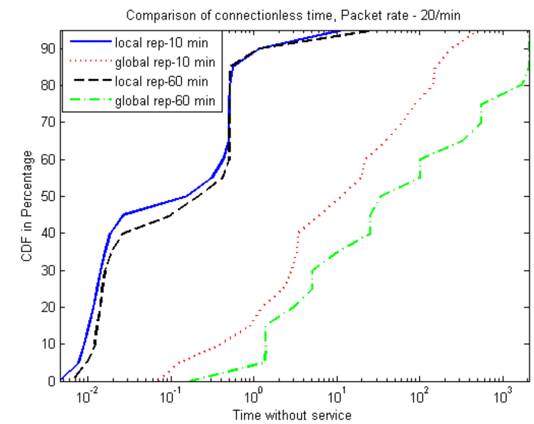

Figure 19: CDF: Comparing loss of connectivity for global repair and global+local repair, packet rate 20/s.

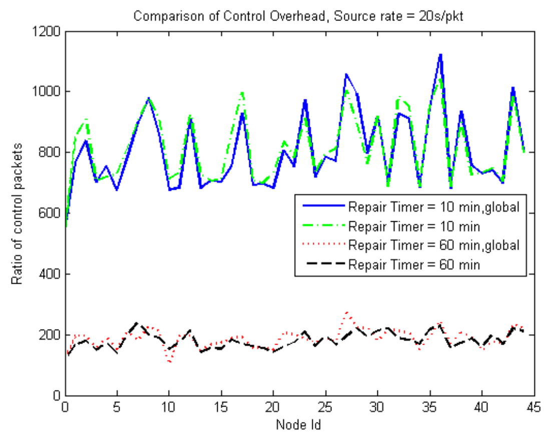

Figure 20: Number of control packets for different DAG Seq Number period, for both global repair and poisoning.

5 RPL in a building automation routing scenario

Unlike the previous traffic pattern, where a majority of the total traffic generated by any node is destined to the root, this section considers a different traffic pattern, which is more prominent in home or building routing scenario. In the simulations shown below, the nodes send 60% of their total generated traffic to the physically 1-hop distant nodes, 20% of traffic to 2-hop distant nodes (again this is a typical traffic pattern in building and home automation networks). The other 20% of the traffic is distributed among all other nodes in the network. The CDF of average hop distance path stretch in terms of hop distance, ETX path cost and delay for P2P routing for all pair of nodes is calculated. The delay bound is more important in this scenario, as the applications in home and building routing have typically low delay tolerance.

5.1 Path Quality

Figure 21 shows the CDF of number of hops for both RPL and ideal shortest path routing for the traffic patttern described above. Figure 22 shows CDF of the expected number of transmission (ETX) for each packet to reach destination. Figures 23 and 24 show CDF of the stretch factor for these two metrics To illustrate the stretch factor, an example from figure 24 will be given next. For all the paths built by RPL, 85% of the time the path cost is less than the path cost for the ideal shortest path plus one.

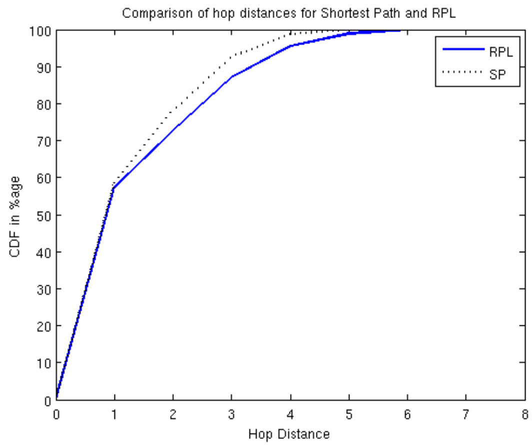

Figure 21: Comparison of end-to-end hop distance for RPL and ideal shortest path in home routing.

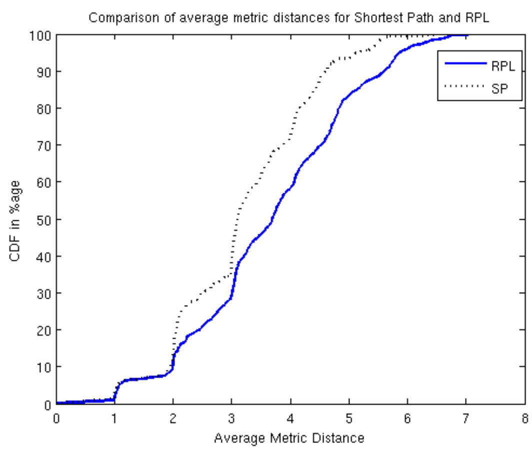

Figure 22: Comparison of path ETX metric for RPL and ideal shortest path in home routing.

5.2 Delay

To get an idea of maximum observable delay in the mentioned traffic pattern, the delay for different number of hops to the destination for RPL is considered. Figure 25 shows how the end-to-end packet latency is distributed for different packets with different hop counts in the network.

6 RPL in a Large Scale Network

In this section we focus on simulating how RPL operates in a large network and study its scalability by focusing on a few performance metrics: the latency, and path cost stretch for performance and the amount of control packets for scalability. The 2442 node smart meter network with its corresponding link traces is used in this scalability study. We also use the corresponding gathered link traces to simulate the packet drop pattern in the network. To simulate a more realistic scenario for a smart meter network, 100% of the

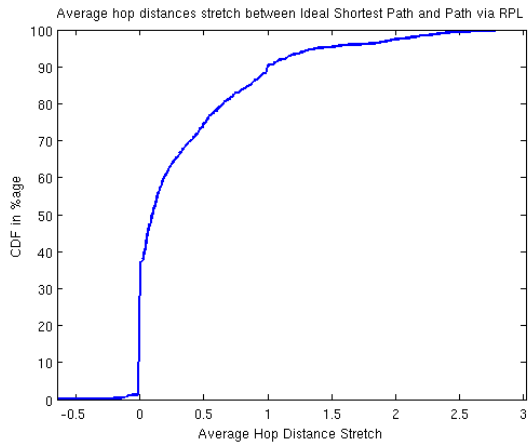

Figure 23: Stretch factor for node hop distance from ideal shortest path.

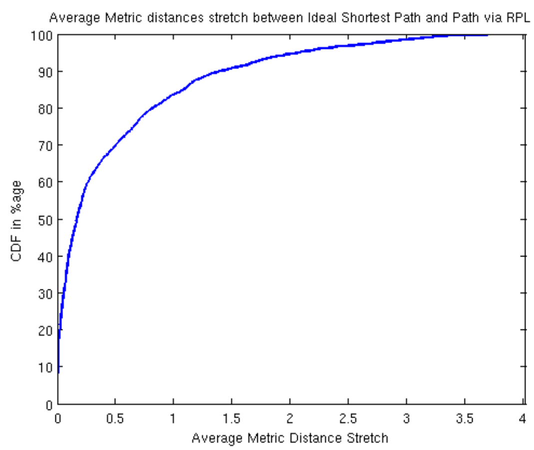

Figure 24: Stretch Factor of total path ETX Metric from ideal shortest path.

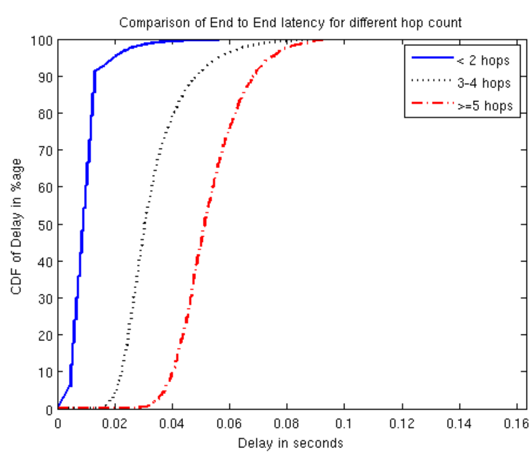

Figure 25: Comparison of packet latency for different hop count in RPL.

generated packets by each node are destined to the root.Therefore, no traffic is destined to nodes other than the root.

6.1 Path Quality

To investigate RPL's scalability, the Cumulative Distribution Function (CDF) of ETX path cost in the large scale smart meter network is compared to an ideal hypothetical shortest path routing protocol which minimizes the total path ETX (Figure 26). In this simulation, the path stretch is also calculated for each packet that traverses the network. The path stretch is determined as the difference between the path ETX taken by a packet while following a route built via RPL and a path computed using an ideal shortest path routing protocol. Here, the CDF of fractional path stretch, which is determned as the path stretch value over the path cost of an ideal shortest path, is plotted in Figure 27. The same fractional path stretch value for hop distance is shown in Figure 28.

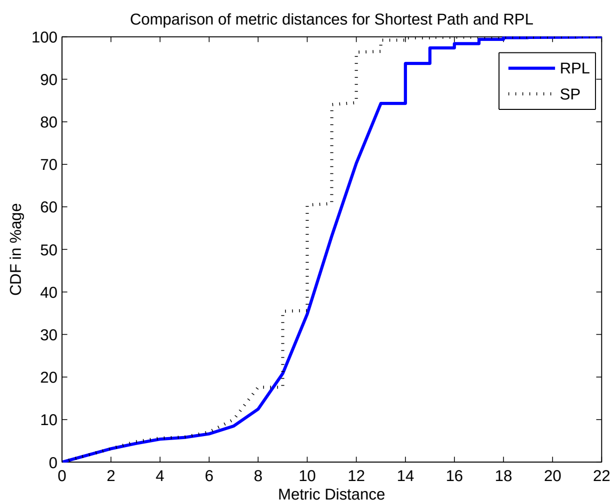

Figure 26: CDF of total ETX path cost

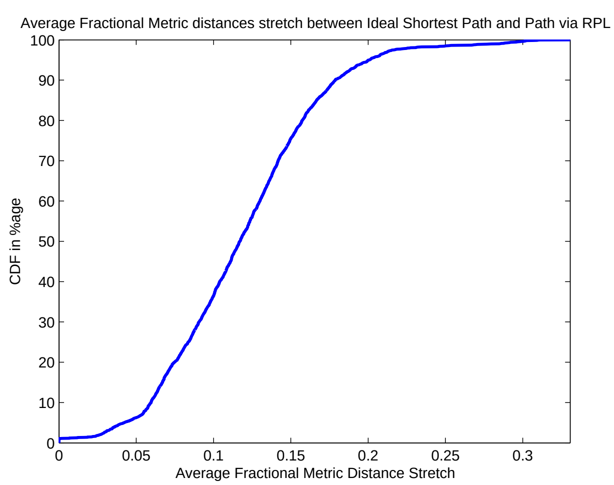

Figure 27: CDF of fractional stretch in ETX path cost

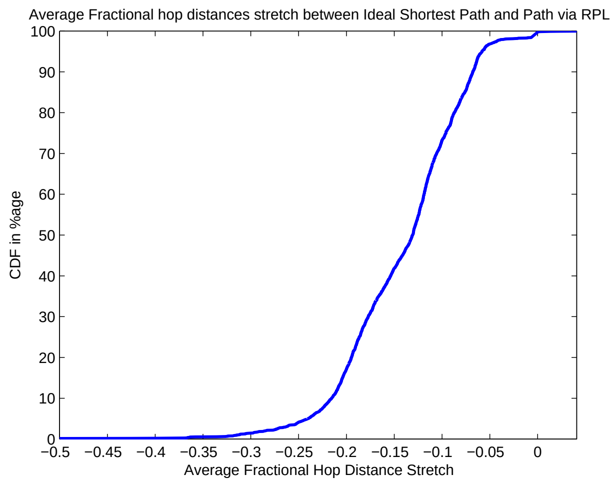

Figure 28: CDF of fractional stretch in hop count

6.2 Delay

Figure 29 shows how the end-to-end packet latency distributed for different packets with different hop counts in the network.

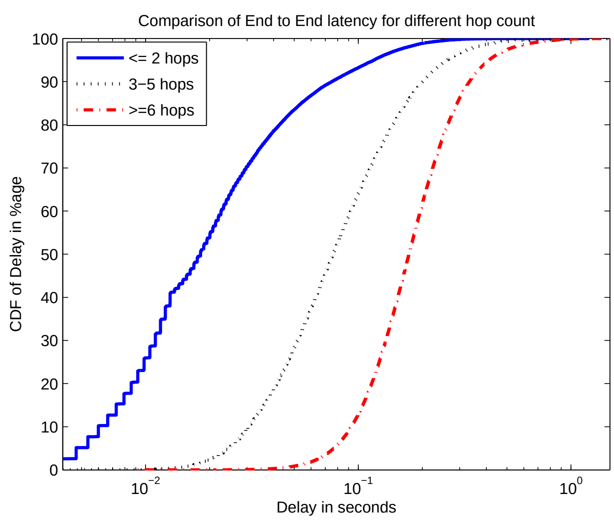

Figure 29: End-to-end packet delivery latency for different hop count

6.3 Control Packet Overhead

Figure 30 shows the comparison between data packets (originated and forwarded) and control packets (DIO and DAO messages) transmitted by each node (link ETX is used as the routing metric). Here one can observe that in spite of the large scale of the network, the amount of control traffic in the protocol is really negligible in comparison to data packet transmission. The smaller node id for this network actually indicates closer proximity to the sink and nodes with high ID are actually further away from the sink. Also, as expected, we can observe on Figures 31, 32, 33 that the (non-leaf) nodes closer to the sink have much more data packet transmission than other nodes. The leaf nodes have comparable amount of data and control packet transmission, as they do not take part in routing the data. As seen before, the data traffic for a child node has much less variation than the nodes which are closer to the sink. This variation decreases with increase in DAG depth. In this topology, nodes 1, 2 and 3, etc. are direct children of the LBR.

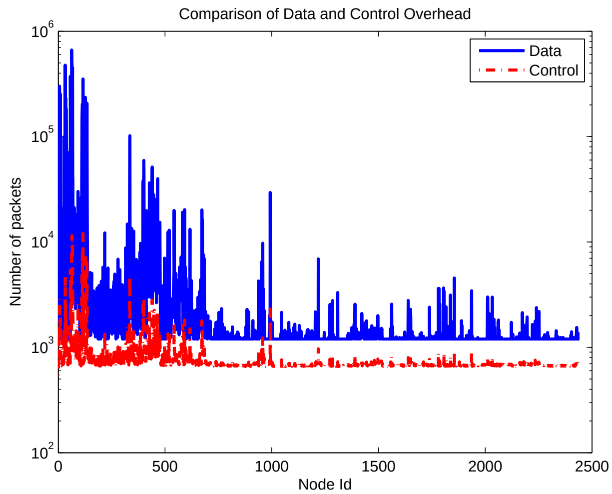

Figure 30: Data and control packet comparison

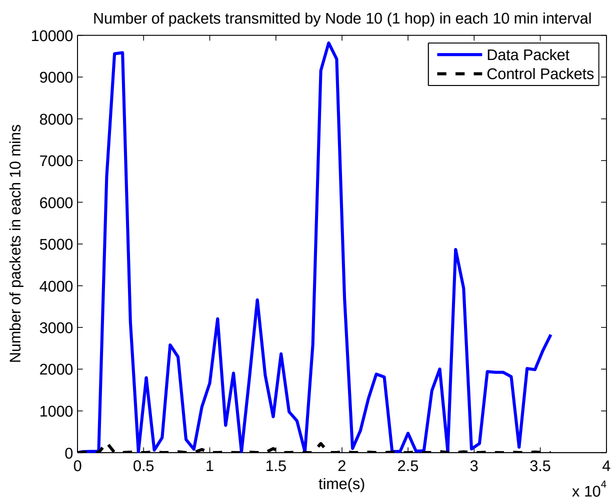

Figure 31: Data and control packet over time for Node 1

In Figure 34, the effect of global repair period timer on control packet overhead is shown.

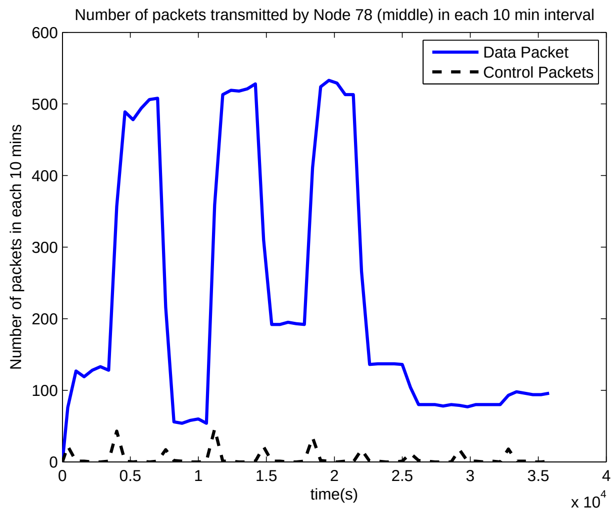

Figure 32: Data and control packet over time for Node 78

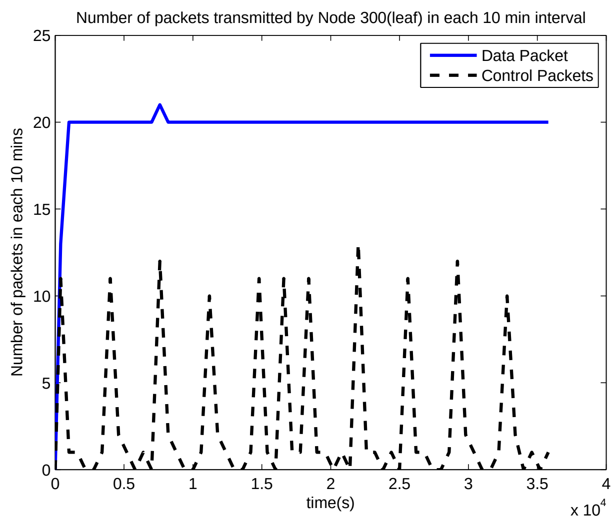

Figure 33: Data and control packet over time for Node 300

7 Scaling Property and Routing Stability

An important metric of interest is the maximum load experienced by any sensor node (CPU usage) in terms of number of the control packets transmitted by the node. Also, to get an idea of scaling properties of RPL in large scale networks, it is also key to analyze the number of packets handled by the RPL nodes for different sizes of the network.

In these simulations, at any given interval, the node with maximum control overhead load is identified. In this draft, the amount of maximum control overhead processed by that node is plotted against time for three different networks under study. The first one is Network 'A', which has 45 nodes and is shown in figure 1 in section 3 ; Network 'B', which is another deployed outdoor network with 86 nodes; and finally, Network 'C', which is the large deployed smart meter network with 2442 nodes being considered in this document.

In Figure 35, the comparison of maximum control load is shown for different network sizes.

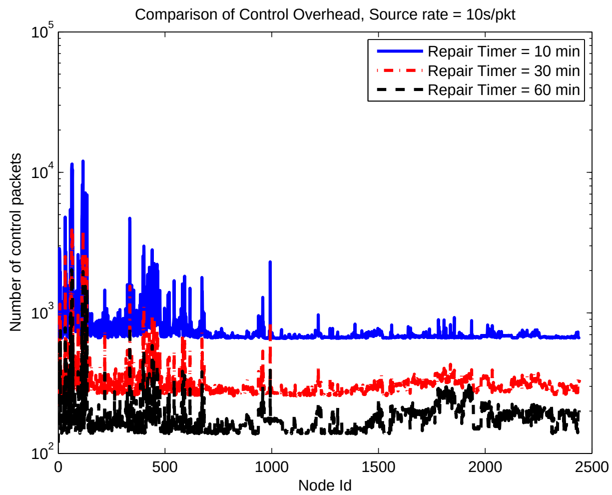

Figure 34: Amount of control packet for different global repair timer period

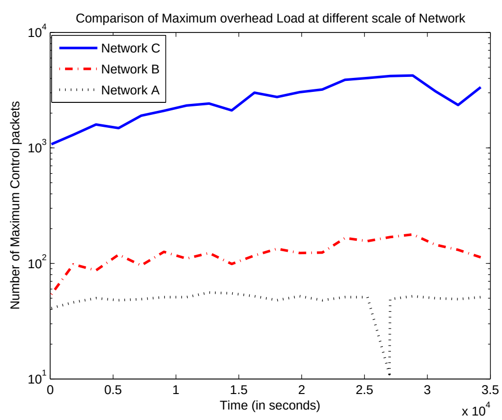

Figure 35: Scaling property of maximum control packets processed by any node over time.

For a network built with low power devices interconnected by lossy links, it is of the utmost importannce to ensure that the routing packets are not flooded in the entire network, and that the routing topology stays as stable as possible. Any change in routing information, specially parent-child relationship, would reset the timer leading to emitting new DIOs, and hence, change the node's path metric to reach the root. This change will trigger a series of control place messages (RPL packets) in the sub-DAG. Therefore, it is important to carefully control the triggering of DIO control packets via the use of thresholds.

In this study, the effect of the tolerance value befored emitting new DIO reflecting a new path cost is analyzed. Four cases are considered in this study

- No change in DAG depth of a node is ignored.
- The implementation ignores 10% of change in the ETX path cost to the root.That is, if the change in total path cost to LBR, due to a DIO reception from most preferred parent or due to shifting to another parent, is less than 10%, the node will not advertise the new metric to the root,
- The implementation ignores 20% change in the path cost to the root for any node before deciding to advertise a new depth, and

- The implementation ignores 30% change in the path cost to the root for any node before deciding to advertise a new depth.

This decision does affect the optimum path quality to the root. As observed in Figure 36, for 0% tolerance, 95% of paths used have a stretch factor less than 10%. Similarly, for 10% and 20% tolerance level, 95% of paths will have a 15% and 20% fractional path stretch. However, the increased routing stability and decreased control overhead is the profit gained from the 10% extra increase in path length or ETX, whichever is used as the metric to optimize DAG.

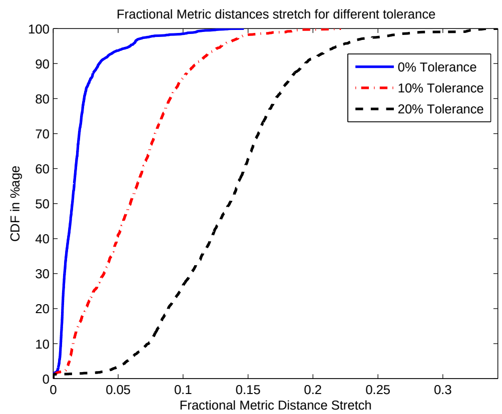

Figure 36: Fractional stretch factor for different tolerance levels

As the above mentioned threshold also affects the path taken by a packet, this study also demonstrates the effect of the threshold on routing stability (number of times P2P paths are changed between a source and a destinaton). For Network 'A' shown in Figure 1 in section 3 and the large smart meter nework 'C', the CDF of path change is plotted against fraction of path change for different thresholds triggeering the emission of a new DIO upon path cost changes.

In Figures 37 and 38, we show the CDF of fraction of times a path has changed (for each source-destination pair) in X axis. If X packets are transferred from source A to destination B, and out of X times, Y times the path between this source-destination pair is changed, then we compute the fraction of path change as $Y/X * 100\%$. this metric is computed over all source-destination pairs, and the CDF is plotted in the Y axis.

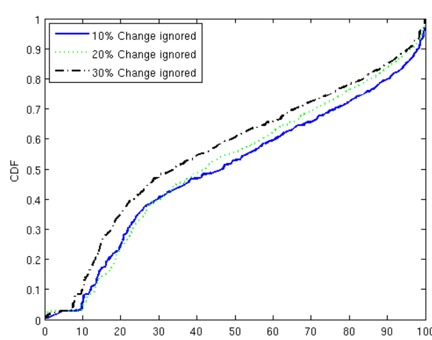

Figure 37: Distribution of fraction of path change, Network 'A'

This document also compares the CDF of fraction of path change for three different networks, 'A', 'B'

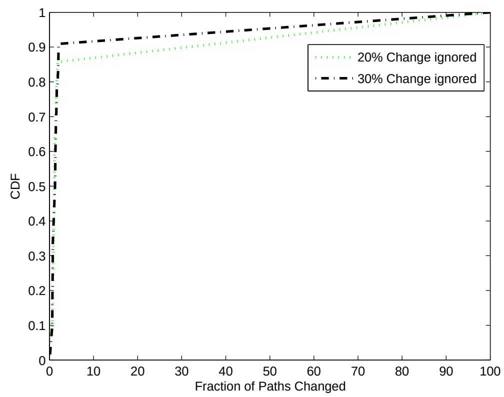

Figure 38: Distribution of fraction of path change, large Network 'C'

and 'C'. Figure 39 shows how the three networks exhibit change of P2P path when 30% change in metric cost to the root is ignored before shifting to a new parent.

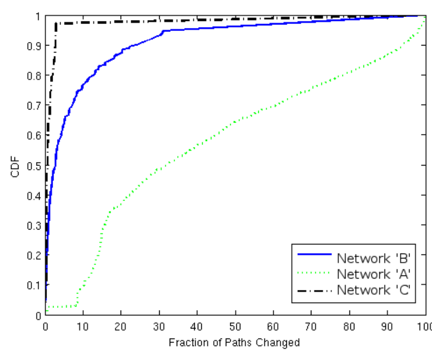

Figure 39: Comparison of distribution of fraction of path change

8 References

8.1 Normative References

[RFC2119] Bradner, S.,“Key words for use in RFCs to Indicate Requirement Levels”, BCP 14, RFC 2119, March 1997.

8.2 Informative References

[RFC5867] Martocci, J., Riou, N., Mil, P., and W. Vermeylen, “Building Automation Routing Requirements in Low Power and Lossy Networks, draft-ietf-roll-building-routing-reqs-07 (work in progress)”, September 2009.

[RFC5826] Brandt, A., Buron, J., and G. Porcu, “Home Automation Routing Requirements in Low Power and Lossy Networks, draft-ietf-roll-home-routing-reqs-08 (work in progress)”, September 2009.

[RFC5873] Pister, K., Thubert, P., Dwars, S., Phinney, T., “Industrial Routing Requirements in Low Power and Lossy Networks, draft-ietf-roll-indus-routing-reqs-06 (work in progress)”, June 2009.

[I-D.ietf-roll-routing-metrics] Vasseur, JP, Kim, M., Pister, K., Chong, H., “Routing Metrics used for Path Calculation in Low Power and Lossy Networks, draft-ietf-roll-routing-metrics-04 (work in progress)”, December 2009.

[I-D.ietf-roll-rpl] Winter, T., Thubert, P., et al., “RPL: Routing Protocol for Low Power and Lossy Networks, draft-ietf-roll-rpl-04 (work in progress)”, November 2009.

[I-D.ietf-roll-terminology] JP Vasseur, “Terminology in Low power And Lossy Networks, draft-ietf-roll-terminology-02 (work in progress)”, May 2009.

[NS-2] “The Network Simulator-2”.

[OMNETpp] Varga, “The OMNeT++ Discrete Event Simulation System”, June 2001.

[RFC5548] Dohler, M., Watteyne, T., Winter, T., and D. Barthel, “Routing Requirements for Urban Low-Power and Lossy Networks”, RFC 5548, May 2009.

[draft-iphc] J. Jurski, “Limited IP Header Compression over PPP, draft-jurski-pppext-iphc-02.txt (work in progress)”, March 2007.

Authors’ Addresses

Joydeep Tripathi (editor) Drexel University
3141 Chestnut Street 7-313
Philadelphia, PA 19104
USA

Email: jt369@drexel.edu

Jaudelice C. de Oliveira (editor)
Drexel University
3141 Chestnut Street 7-313
Philadelphia, PA 19104
USA

Email: jau@ece.drexel.edu

JP Vasseur (editor)
Cisco Systems, Inc.
1414 Massachussetts Avenue
Boxborough, MA 01719
USA

Email: jpv@cisco.com